Partial Symmetrization of the Photosynthetic Reaction Center

STEVEN J. ROBLES, JACQUES BRETON, DOUGLAS C. YOUVAN

The bacterial photosynthetic reaction center (RC) is a pigmented intrinsic membrane protein that performs the primary charge separation event of photosynthesis, thereby converting light to chemical energy. The RC pigments are bound primarily by two homologous peptides, the L and M subunits, each containing five transmembrane helices. These α helices and pigments are arranged in an approximate C_2 symmetry and form two possible electron transfer pathways. Only one of these pathways is actually used. In an attempt to identify nonhomologous residues that are responsible for functional differences between the two branches, homologous helical regions that interact extensively with the pigments were genetically symmetrized (that is, exchanged). For example, replacement of the fourth transmembrane helix (D helix) in the M subunit with the homologous helix from the L subunit yields photosynthetically inactive RCs lacking a critical photoactive pigment. Photosynthetic revertants have been isolated in which single amino acid substitutions (intragenic suppressors) compensate for this partial symmetrization.

A CENTRAL PROBLEM IN BIOPHYSICS is to determine the mechanism by which amino acid residues in proteins mediate efficient and highly directional electron transfer between bound prosthetic groups. We have addressed this question by studying a protein which possesses two possible electron transfer pathways but uses only one. In the photochemical core of the bacterial RC (Fig. 1), chemically equivalent redox centers are arranged about an approximate C_2 symmetry axis running from a special pair (P) of bacteriochlorophyll molecules to a ferrous iron ion (*1–4*). The first spectroscopically resolved charge-separation event involves electron donation from the excited singlet state of P (*5*) to the bacteriopheophytin that is more closely associated with the L subunit, H_A (*6*). The possible involvement of a reduced intermediate of B_A, a bacteriochlorophyll situated between these chromophores, is uncertain at present (*7*). In the second electron transfer step, H_A^- transfers an electron to the primary quinone Q_A, which subsequently transfers the electron across the axis of symmetry to the secondary quinone, Q_B.

The C_2 axis of the RC is considered approximate because superposition (graphic rotation) of the active ("A") branch prosthetic groups onto the opposite ("B") branch shows some structural differences. Ultimately, these deviations from perfect symmetry should be traceable to primary sequence differences between the L and M subunits, which provide the binding pockets for the pigments.

Because of the high degree of sequence identity between the L and M subunits, it has been proposed (*8*) that their genes may have arisen from a common ancestor. This hypothesis has the interesting implication that the ancestral subunit "X" may have existed within a fully symmetric RC consisting of an X_2 homodimer rather than an LM heterodimer. Extending this hypothesis (*4*), divergent sequences were selected that make the light reactions more efficient (i) by optimizing only one of the two pathways for the primary charge separation reactions and (ii) by specializing the function of the two RC quinones. The first quinone to be reduced (Q_A) is tightly bound and functions as a one-electron carrier, whereas the second quinone (Q_B) is loosely bound and functions as a mobile two-electron gate.

In order to test the homodimer hypothesis and, more generally, to study the structures responsible for unidirectional electron transfer, we used molecular genetics to artificially symmetrize RCs. In previous experiments, RCs have been symmetrized by modifying single residues thought to be important for unidirectionality (*6*). To date, no single residue has been found that determines the directionality of electron transfer (*9*). Thus it seems reasonable to address the problem through more global rearrangement (such as symmetrization) of larger sections of the protein. In such constructions, poorly understood biogenesis and protein folding pathways must be considered that prevent the formation of L-subunit or M-subunit homodimers. Excluding possible effects of other peptides bound to the core of the RC, such fully symmetrized RCs might be expected to carry out bidirectional electron transfer in a manner similar to their putative X_2 ancestor.

As a first step in this direction, we investigated whether genetically engineered RCs can be constructed wherein structurally important segments of the protein are duplicated or exchanged between the L and M subunits, thus effecting a partial symmetrization or reversal of asymmetry, respectively. For these initial studies, the D helices were chosen because they contain the shortest contiguous sequences that provide important binding interactions for all nine of the prosthetic groups. Successful symmetrization of the D-helix sequence in both subunits sets a lower limit on the amount of primary sequence that can be transplanted from one subunit to the other before structural factors prevent assembly of a stable protein.

The L- and M-subunit genes were separately subcloned into M13 derivatives and unique Bst EII and Nsi I restriction sites were engineered at each end of the regions encoding the D helices. These homologous sites were used to exchange or duplicate the two D helices. Each region encodes 26 amino acid residues, 13 of which differ between the two subunits (Fig. 2). One of the engineered sites, Bst EII at sequence position L167, required a point mutation that changed a Phe residue to Leu. In the RC x-ray structure from *Rhodopseudomonas viridis*, this residue is a Trp that appears to be in van der Waals contact with P_A, one of the bacteriochlorophyll molecules in the special pair. In *Rhodobacter capsulatus*, this mutation at L167 does not appear to affect photosynthetic growth, but results in a 20-nm blue shift of the Q_Y band of P in the RC spectra.

The subclones containing the D-helix substitutions were reassembled into plasmid pU2924 (encoding the *puf*-operon) (*10*). The mutant designated "D_{LL}" has the M-subunit D helix replaced with the homologous region from the L subunit, mutant "D_{MM}" has the L-subunit D helix replaced by the M sequence, and mutant "D_{LM}" has the two D helices switched. Of these three mutants, only D_{MM} exhibits photosynthetic growth (PS^+), although it appears to be severely impaired relative to wild type. Freshly prepared membranes from the D_{MM} and D_{LM} mutants have absorption spectra characteristic of RCs (absorbance at 800 and 860 nm); however, these signals degenerate within hours. These membranes also exhibit a large absorbance peak at 770 nm, indicative of free pigments, which precludes a more detailed spectroscopic characterization at present. However, RCs from the D_{LL} mutant appear to be stable in chromatophore membranes (not solubilized in

S. J. Robles, Graduate Program in Applied Biological Sciences, Massachusetts Institute of Technology, Cambridge, MA 02139.
J. Breton, Service de Biophysique, Département de Biologie, CEN Saclay, 91191 Gif-sur-Yvette Cedex, France.
D. C. Youvan, Department of Chemistry, Massachusetts Institute of Technology, Cambridge, MA 02139.

detergent), which can be purified by sucrose density centrifugation from a background strain [U43(pU2924:Ala$^{\alpha 28}$ → Glu)]. Membranes from this strain lack all light-harvesting complexes but express RCs. This new genetic background facilitates in situ optical spectroscopy on membrane-bound RCs that are unstable because of structural alterations (*11*).

The absence of the 545-nm and 754-nm peaks in the 10 K absorbance and linear dichroism (LD) spectra of the D_{LL} mutant chromatophores (Fig. 3) strongly suggests that D_{LL} RCs lack H_A, the intermediate electron acceptor (*12*). Having generated this mutant, it may now be possible to use it for several important spectroscopic measurements (i) to clarify the role of B_A in the initial charge-separation event, (ii) to measure the spectrum and lifetime of the excited state of the special pair, and (iii) to detect "wrong-way" electron transfer to H_B (*13*).

In *Rb. capsulatus*, photosynthetically defective (PS^-) mutants can be grown under chemoheterotrophic conditions. Classical selection techniques can be used to obtain a large dynamic range of photosynthetically competent revertants. Some revertants grow only under extremely high light levels, while others grow well in very low light. PS^+ revertants can be ranked in a hierarchy dependent on the dose of light (intensity times time) required for growth.

We used photosynthetic growth to select spontaneous revertants for the D_{LL} and D_{MM} mutants that restore or enhance photosynthetic growth (designated PS↑↑). Sequence changes found in the PS↑↑ revertants are listed in Table 1. Despite numerous attempts (involving repeated and serial subculturing of precultures), no PS↑↑ revertants of the D_{LM} mutant were obtained. This result suggests that more than one or two point mutations are needed to restore photosynthetic growth in the D_{LM} mutant.

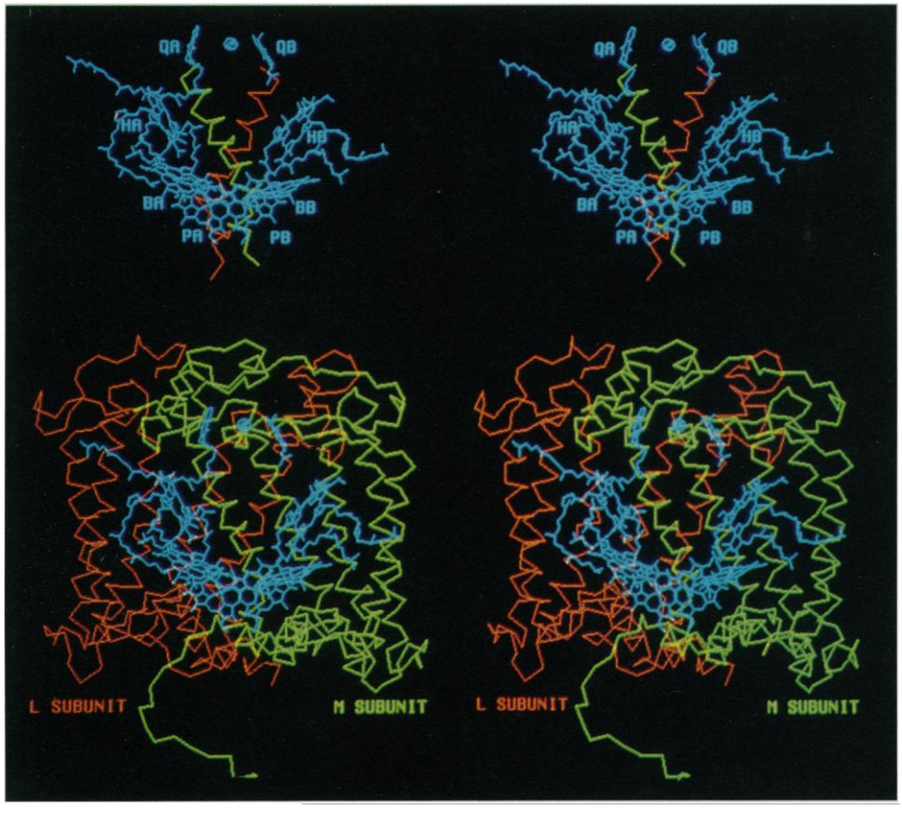

Fig. 1. (**Top**) Stereo view of the RC prosthetic groups and the α-carbon backbone of the transmembrane D helices from the L subunit (displayed in red) and from the M subunit (displayed in green). Only the regions involved in the construction of the D_{LL}, D_{MM}, and D_{LM} mutants are shown. Prosthetic groups (blue) are labeled according to the convention of whether they lie on the photoactive "A" branch or the opposite "B" branch. The two bacteriochlorophyll molecules comprising the special pair (P) are labeled P_A and P_B. The monomeric bacteriochlorophyll molecules are labeled B_A and B_B, and the bacteriopheophytin molecules are labeled H_A and H_B. The primary quinone is labeled Q_A and the secondary quinone is labeled Q_B. A ferrous iron ion lies between the two quinone molecules on the pseudo C_2 symmetry axis, which runs vertically in the plane of the figure. (**Bottom**) The L and M subunits of the RC of *R. viridis* are shown in their entirety in exactly the same orientation used in the upper stereo pair. An x-ray crystallographic structure has also been published for RCs from *Rb. sphaeroides*, which is similar to the *R. viridis* (*1–4*) structure. Although a structure is not yet available for the RC of *Rb. capsulatus*, the protein sequences are highly homologous and the spectroscopy and photochemistry are nearly identical for RCs from these three species (*7, 12, 16*). *Rhodobacter capsulatus* is the preferred organism for these studies, since it is well characterized genetically and is easily manipulated (*9, 17*). Unless otherwise indicated, references to the RC structure are to *R. viridis*, which has been refined to 2.3 Å resolution (*4*).

Several of the PS↑↑ D_{LL} revertants show additional mutations at positions M212 and M216. Those occurring at M216 are actually compensatory mutations, unlike those at M212, which are reversions to the original wild-type residue. Two of the PS↑↑ D_{LL} revertants (designated D_{LL}7b and D_{LL}7c) have been characterized by absorbance and LD spectroscopy at 10 K in light-harvesting free membranes. In both revertants, the 754-nm absorption band assigned to the intermediate electron acceptor H_A reappears. However, in the D_{LL}7b revertant this absorption band has ~30% of the amplitude found in the wild type, whereas in D_{LL}7c it is blue-shifted to 750 nm.

Two different types of revertants with enhanced photosynthetic growth (PS↑↑) were isolated from the D_{MM} mutant. The spectra indicate the absence of the 742-nm band and the presence of a 754-nm band characteristic of an intermediate electron acceptor. This result suggests that RCs from these revertants are possible candidates for bidirectional electron transfer. One revertant (strain D_{MM}3h) was identified at position L187, which, according to the x-ray structure of *R. viridis*, is in the vicinity of H_B. Another PS↑↑ revertant (strain D_{MM}3g) occurs within the E helix of the L subunit at position L237, which is near H_A. Surprisingly, a Pro residue now appears in this transmembrane helix. The mutation could enhance protein stability by altering the tertiary structure to compensate for molar volume losses in D_{MM}.

Molar volume differences may also account for several of the other revertant mutations leading to PS↑↑ phenotypes. The D_{LL} RC has a total side-chain molar volume that is 178 Å^3 greater than that of wild type (*14*). This overpacked structure could be responsible for preventing bacteriopheophytin from occupying the H_A site. All of the PS↑↑ D_{LL} revertants have mutations that decrease the molar volume at residues near H_A.

The position of these PS↑↑ reversions indicates that the region around the bacteriopheophytins is the most sensitive to defects in assembly or stability or both that are induced by helix duplication. This observation is consistent with previous analysis of the crystal structure data, which show that the chromophores increasingly deviate from C_2 symmetry as one moves from P to H (*1, 4*).

PS↑↑ revertants of the D-helix duplica-

Table 1. Genotypes of several enhanced photosynthetic growth ($PS^{\uparrow}$) revertants isolated from parental strains in which the RC genes have been partially symmetrized. Primary site reversions restore the sequence of the wild type at a given sequence position, whereas second site suppressor mutations make use of novel sequences not found in either subunit at the homologous sequence positions. Sequence positions are numbered according to the convention that the transplanted helix assumes the numbering system of the recipient subunit. Since independent precultures were used for the isolation of the $PS^{\uparrow}$ revertants, the number of independent isolates is significant (*19*). All of the primary site reversions and secondary site intragenic suppressors listed in this table (with the exception of the four isolates of $Phe^{L187} \rightarrow$ Leu) lie close to the photoactive bacteriopheophytin. Two different Leu codons (TTA and CTC) were found to be used in the four independently isolated $Phe^{L187} \rightarrow$ Leu revertants. Qualitative photosynthetic growth assays performed as "spot" inocula on petri dishes incubated under high light conditions (~10 mW cm^{-2}) reveal the following hierarchy in growth rates; wild type > D_{LL}7d, D_{LL}7b, D_{MM}3h > D_{MM}3g > D_{MM} > D_{LL}7e, and D_{LL}7c; no growth detected for D_{LL} and D_{LM}.

Revertant strain	Parent strain	Primary site reversion	Secondary site suppressor	Number of independent isolates
D_{LL}7b	D_{LL}	$Trp^{M212} \rightarrow$ Leu	None	2
D_{LL}7d	D_{LL}	$Trp^{M212} \rightarrow$ Leu	$Ile^{M204} \rightarrow$ Thr	1
D_{LL}7e	D_{LL}	None	$Met^{M216} \rightarrow$ Val	2
D_{LL}7c	D_{LL}	None	$Met^{M216} \rightarrow$ Thr	2
D_{MM}3h	D_{MM}	$Phe^{L187} \rightarrow$ Leu	None	4
D_{MM}3g	D_{MM}	None	$Ala^{L237} \rightarrow$ Pro	1

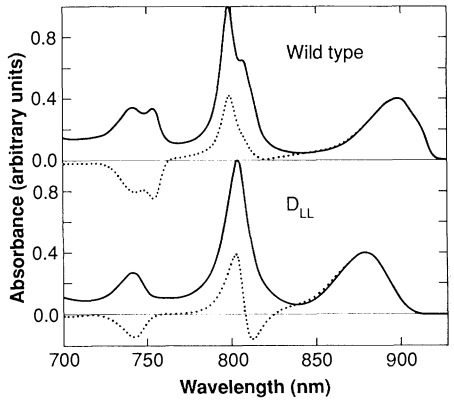

Fig. 3. In situ ground-state absorption (——) and linear dichroism (------) spectra (10 K) of oriented chromatophore membranes from strain U43(pU2924:$Ala^{\alpha 28} \rightarrow$ Glu) expressing RCs as the only detectable pigmented protein (*11*). (**Top**) Chromatophores bearing wild-type RCs. (**Bottom**) D_{LL} mutant chromatophores wherein the M-subunit D helix has been replaced by the homologous helix from the L subunit. The complete disappearance of the Q_Y transitions of H_A at 754 nm as well as the Q_X transition at 545 nm indicates that the intermediate electron acceptor H_A is absent in the D_{LL} mutant. The shoulder observed at 807 nm for RCs from wild type (absent in the spectrum of the D_{LL} mutant) is thought to contain contributions from both B_B and the high-energy exciton component of the special pair (P_{Y+}), in addition to B_A, whose main peak is located at 799 nm in the wild-type sample (*12*). In the D_{LL} mutant this main peak is shifted to 804 nm, where it coalesces with the band from B_B. This shift is probably due to enhanced symmetry in the environment of the two monomeric bacteriochlorophylls. The LD spectra fully support these chromophore assignments for both wild-type and D_{LL} RCs. A difference in the overlap between the positive contributions from the Q_Y transitions of B_A and B_B and the negative contribution from P_{Y+} is sufficient to explain the LD spectra in the 805- to 820-nm region. In addition, the LD spectra in both the Q_Y and Q_X regions demonstrate that the relative orientations of the five remaining chromophores in the D_{LL} mutant are essentially unperturbed compared to wild type.

tions differ from wild type by 11 to 14 amino acid residues, and some of these residues are thought to participate in important structural interactions with the chromophores. For example, Tyr M208 (replaced by Phe in the D_{LL} mutant) forms a hydrogen bond to the 7c-carbonyl of the propionic group of P_A in *Rhodobacter sphaeroides* (*2*). This residue is situated between P, B_A, and H_A, and is speculated to be involved in the initial charge separation event. None of the $PS^{\uparrow}$ revertants of the D_{LL} mutant we have isolated show reversion to Tyr at this site, demonstrating that Tyr M208 is not essential for charge separation.

Other interesting pairs of amino acid residues shown in Fig. 2 include His L168 (which forms a hydrogen bond with the acetyl group of P_A near B_B) and the symmetry-related Phe at M195 near P_B and B_A. Another residue, Ser L178, hydrogen bonds to the oxygen of the 7c-carbonyl of B_B in the *Rb. sphaeroides* structure and may therefore be involved in altering the position of the phytyl chain of B_B (*15*). This effect could inhibit electron transfer along the B branch. Since the $PS^{\uparrow}$ revertants of D_{LL} and D_{MM} mutants lack these wild-type residues, none of these residues can be absolutely essential for charge separation. Furthermore, no $PS^{\uparrow}$ revertant mutations were found at any of these critical positions. However, the $PS^{\uparrow}$ revertants are photosynthetically impaired, thus, whereas the residues cited above are not absolutely essential for photosynthesis, some probably optimize RC photochemistry to a significant extent.

We have genetically altered the bacterial photosynthetic RC such that 2 of the 11 transmembrane α helices extensively involved in pigment binding have been either exchanged or duplicated. These large-scale structural rearrangements result in defects in protein folding or electron transfer or both that can be compensated by single point mutations. Absorption and LD spectra of the modified pigment proteins have been obtained directly from membranes lacking all other chromophores. Duplication of the L-subunit D helix results in the loss of the photoactive bacteriopheophytin without significant perturbation of the other prosthetic groups. Photosynthetically competent revertants of the D helix duplications can be spectroscopically probed for bidirectional electron transfer. Partially symmetrized RCs are important because they constrain structure-function models that invoke essential amino acid asymmetries between the L and M subunits for charge separation. Useful constructions that could be made on other sections of the RC subunits, adjacent to the D helices, include the amphipathic cd helices

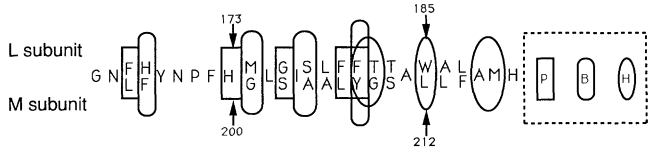

Fig. 2. Amino acid sequence of the transmembrane D helices from *Rb. capsulatus*, in the region analogous to the α-carbon backbone displayed in the upper stereo pair of Fig. 1. Thirteen sequence differences between the L subunit [(**top**) residues Gly^{165} through His^{190}] and M subunit [(**bottom**) residues Gly^{192} through His^{217}] are listed as vertical pairs, respectively. The key within the dashed box at the right indicates the interaction of these amino acid positions with the special pair bacteriochlorophylls (P), monomeric bacteriochlorophylls (B), and the bacteriopheophytins (H). According to the high-resolution x-ray structure of *R. virdis*, the conserved residues His^{L173} and His^{M200} are the axial ligands to the central Mg atoms of P_A and P_B, respectively; His^{L190} and His^{M217} are two of the five amino acid residues binding Fe^{2+}; Met^{L185} and Leu^{M212} approach closest to the centers of H_B and H_A, respectively; Leu^{L187} and Phe^{M214} are one-half turn of the helix away from these bacteriopheophytins (*4*). All of these residues are conserved between *R. viridis* and *Rb. capsulatus*, with the exception of Met^{L185}, which is Trp^{L185} in *Rb. capsulatus*. The sequence differences observed between *Rb. capsulatus*, *Rb. sphaeroides*, and *R. viridis* are summarized in (*18*). In comparison to Fig. 1, one may note that the D helices cross each other, such that the L-subunit D helix interacts primarily with P_A and H_B, whereas the M-subunit D helix interacts primarily with P_B and H_A. Abbreviations for the amino acid residues are: A, Ala; C, Cys; D, Asp; E, Glu; F, Phe; G, Gly; H, His; I, Ile; K, Lys; L, Leu; M, Met; N, Asn; P, Pro; Q, Gln; R, Arg; S, Ser; T, Thr; V, Val; W, Trp; and Y, Tyr.

that bind B_A and B_B, and the regions between the D and E helices that form most of the Q_A and Q_B binding sites.

REFERENCES AND NOTES

1. H. Michel, O. Epp, J. Deisenhofer, *EMBO J.* **5**, 2245 (1986).
2. J. P. Allen, G. Feher, T. O. Yeates, H. Komiya, D. C. Rees, *Proc. Natl. Acad. Sci. U.S.A.* **84**, 5730 (1987); *ibid.* **85**, 8487 (1988); C.-H. Chang *et al.*, *FEBS Lett.* **205**, 82 (1986).
3. J. Deisenhofer, O. Epp, K. Miki, R. Huber, H. Michel, *Nature* **318**, 618 (1985).
4. J. Deisenhofer and H. Michel, *Science* **245**, 1463 (1989); *EMBO J.* **8**, 2149 (1989).
5. C. Kirmaier and D. Holten, *Photosynth. Res.* **13**, 225 (1987); J. D. McElroy, G. Feher, D. C. Mauzerall, *Biochim. Biophys. Acta* **172**, 180 (1969); J. R. Norris, R. A. Uphaus, H. L. Crespi, J. J. Katz, *Proc. Natl. Acad. Sci. U.S.A.* **68**, 625 (1971).
6. E. J. Bylina, C. Kirmaier, L. McDowell, D. Holten, D. C. Youvan, *Nature* **336**, 182 (1988).
7. G. R. Fleming, J. L. Martin, J. Breton, *ibid.* **333**, 190 (1988); W. Holzapfel *et al.*, *Chem. Phys. Lett.* **160**, 1 (1989).
8. D. C. Youvan and B. L. Marrs, *Cell* **39**, 1 (1984).
9. W. J. Coleman and D. C. Youvan, *Annu. Rev. Biophys. Biophys. Chem.* **19**, 333 (1990).
10. Plasmid pU2924 is a derivative of pU2922 lacking two Hind III and two Bam HI restriction sites outside the *puf* operon insert [E. J. Bylina, R. V. M. Jovine, D. C. Youvan, *Bio/Technology* 7, 69 (1989)].
11. The *Rb. capsulatus* strain U43 does not express RCs or light-harvesting antennae complexes LH I and LH II. The RC L- and M-subunit genes and the LH I α and β subunit genes had been deleted by interposon mutagenesis [D. C. Youvan, S. Ismail, E. J. Bylina, *Gene* **38**, 19 (1985)]. The $Ala^{\alpha 28} \rightarrow$ Glu substitution at residue 28 of the α subunit gene of LH I was incorporated into plasmid pU2924 [E. J. Bylina, S. J. Robles, D. C. Youvan, *Isr. J. Chem.* **28**, 73 (1988)]. This nomenclature for mutations is used throughout.
12. J. Breton, E. J. Bylina, D. C. Youvan, *Biochemistry* **28**, 6423 (1989); J. A. Abdourakhmanov, A. O. Ganago, Y. E. Erokhin, A. A. Solovev, V. A. Chugunov, *Biochim. Biophys. Acta* **546**, 183 (1979); J. Breton, *ibid.* **810**, 235 (1985); in *The Photosynthetic Bacterial Reaction Center: Structure and Dynamics*, J. Breton and A. Verméglio, Eds. (Plenum, New York, 1988), pp. 59–69.
13. J. Breton, J.-L. Martin, M. E. Michel-Beyerle, S. J. Robles, D. C. Youvan, unpublished results.
14. Molar volume differences were calculated with values taken from A. Z. Zamyatnin, *Prog. Biophys. Mol. Biol.* **24**, 107 (1972).
15. H. Komiya, T. O. Yeates, D. C. Rees, J. P. Allen, G. Feher, *Proc. Natl. Acad. Sci. U.S.A.* **85**, 9012 (1988).
16. C. Kirmaier and D. Holten, *Isr. J. Chem.* **28**, 79 (1988); R. C. Prince and D. C. Youvan, *Biochim. Biophys. Acta* **890**, 286 (1987).
17. P. A. Scolnick and B. L. Marrs, *Annu. Rev. Microbiol.* **41**, 703 (1987).
18. D. M. Tiede *et al.*, in *The Photosynthetic Bacterial Reaction Center: Structure and Dynamics*, J. Breton and A. Verméglio, Eds. (Plenum, New York, 1988), pp. 13–20.
19. Spontaneous revertants were obtained by inoculating liquified medium containing 1.5% agar with a serially subcultured mutant stock, each started from a single purified colony. Samples were incubated at 32°C in 10 mW cm^{-2} white light. PS↑ revertants from the D_{MM} mutant were obtained at lower light intensity, ~1 mW cm^{-2}. PS↑ revertants $D_{LL}7b$ and $D_{LL}7d$ were isolated from liquid cultures grown anaerobically under high light conditions to enhance the probability of multiple reversions.

20. Supported by NSF grant DMB-8609614 and NIH grant R1GM42645A. We thank M. E. Michel-Beyerle and W. J. Coleman for a critical reading of the manuscript.

30 January 1990; accepted 4 May 1990

Correlated Evolution of Female Mating Preferences and Male Color Patterns in the Guppy *Poecilia reticulata*

ANNE E. HOUDE AND JOHN A. ENDLER

Sexual selection may explain why secondary sexual traits of males are so strongly developed in some species that they seem maladaptive. Female mate choice appears to favor the evolution of conspicuous color patterns in male guppies (*Poecilia reticulata*) from Trinidad, but color patterns vary strikingly among populations. According to most theory, correlated evolution of female mating preferences and preferred male traits within populations could promote this kind of divergence between populations. But mating preferences could also constrain the evolution of male traits. In some guppy populations, females discriminate among males based on variation in the extent of orange pigment in male color patterns, and populations differ significantly in the degree of female preferences for orange area. In a comparison of seven populations, the degree of female preference based on orange is correlated with the population average orange area. Thus male traits and female preferences appear to be evolving in parallel.

DARWIN (*1*) SUGGESTED THAT MATE choice by females can lead to the evolution of elaborate sexual display traits. Models of sexual selection (*2–6*) assume genetic variation in female preferences and suggest mechanisms for correlated evolutionary changes in both female preferences and male secondary sexual traits. Female mating preferences affect the evolution of male traits directly. Changes in female preferences may result from direct selection, indirect "good genes" selection (*5, 7*), or correlated effects of selection on other traits or functions. Environmental differences can affect how females perceive males, leading to nongenetic differences in the expression of preferences (*6*). In addition, the Fisher model of sexual selection (*2, 3*) predicts a within-population genetic correlation between female preferences and male traits because females with a particular preference tend to mate nonrandomly with males with the corresponding sexual display traits. This genetic correlation leads to changes in female preferences as an indirect response to selection on male traits, leading in turn to further changes in both characters. Each model predicts correlated evolution of female preferences and preferred male traits within populations. The direction in which male traits and female preferences evolve depends on stochastic and selective factors (such as direct selection on male traits by predators), so different populations are expected to evolve divergent suites of male traits and female preferences (*3, 4*). But it is also possible that female mate choice could limit the divergence of male traits if the evolution of mating preferences is constrained (*8–10*). Female choice for an ancestral type may explain why male butterflies are often nonmimetic in species with mimetic females (*8*), and conserved patterns of mate choice may promote hybridization in some fish species (*9, 10*). There is some evidence for genetic variation in female preferences (*11*), but there is little empirical information on the joint evolutionary dynamics of mating preferences and male secondary sexual traits to evaluate these ideas. We compared mating preferences of female guppies (*Poecilia reticulata*) from natural Trinidad populations that vary greatly in male color patterns to test the idea of parallel divergence in preferences and preferred male traits.

The color patterns of male guppies vary within and between populations, and some of this variation is related to differences in predation regime (*12*). Within populations, females have mating preferences based on variation in male color patterns, particularly orange spots (*7, 12–14*). Data from three streams show that female preferences differ among populations and suggest that male color patterns and female preferences may covary across populations (*15, 16*). We present data on preferences and color patterns from seven populations in six streams (Table 1).

All experiments were conducted with fish descended from individuals collected in Trinidad less than three generations previously and raised under standard conditions (*14*). Virgin females used in our experiments were reared in sibling groups and separated from males before male color patterns developed. Males were reared to maturity in sibling groups and then were allowed to interact with stock females for several days before we used them in experiments. Female choice is based on the relative area of orange pigment in male color patterns (orange area; *17*) and was studied by placing experimental groups of six males and six females in 1.0 by 0.5 by 0.3 m aquaria (with gravel on three

A. E. Houde, Department of Ecology and Evolutionary Biology, Princeton University, Princeton, NJ 08544–1003.
J. A. Endler, Department of Biological Sciences, University of California, Santa Barbara, CA 93106.